Nuclear Physics B280 [FS18] (1987) 289–303
North-Holland, Amsterdam

THE GROSS-NEVEU MODEL AT FINITE TEMPERATURE AND DENSITY

F. KARSCH[1], J. KOGUT and H.W. WYLD

University of Illinois at Urbana-Champaign, Department of Physics, Loomis Laboratory, 1110 W. Green Street, Urbana IL 61801, USA

Received 21 July 1986

The thermodynamics of the Gross-Neveu model is analyzed at finite temperature and finite chemical potential μ on the lattice. The chiral transition is found to be first order for all $\mu > 0$ and second order at $\mu \equiv 0$. The different phases are studied and direct evidence for the creation of a kink-antikink condensate at μ_c is presented.

1. Introduction

It would be of great interest to analyze the phase structure of QCD at finite temperature and density. However, the introduction of a finite chemical potential into the QCD partition function leads to a complex fermion determinant and thus makes a numerical analysis by the standard Monte Carlo techniques difficult. Moreover, quenched calculations for QCD with nonvanishing chemical potential (μ) encounter severe problems [1] which may signal a failure of the quenched approximation at $\mu \neq 0$ [2]. Thus an analysis in the presence of dynamical fermions seems to be mandatory at $\mu \neq 0$. Having in mind these difficulties for QCD it would seem to be helpful to have a model at hand that allows us to test certain concepts of the lattice formulation of field theories with nonvanishing chemical potential [3–5] and to study the approach to the continuum limit. The Gross-Neveu model (GNM) [6] is well suited for this purpose. It is a two-dimensional asymptotically free theory which shows spontaneous breakdown of a (discrete) chiral symmetry. Thus it has many features in common with QCD. In addition, the model is well studied in the continuum [7] and the phase structure at finite temperature [8,9] and density [10] has been analyzed in the large n_f limit. The discussion of the phase structure in the $n_f \to \infty$ limit, however, relies on a mean field approach, which especially for $\mu \neq 0$ may be unreliable since nonuniform field configurations may be important. Thus besides using the GNM to test the lattice formulation of finite density field theories

[1] Address after September 1, 1986: CERN, Theory Division, 1211 Geneva 23, Switzerland.

0619-6823/87/$03.50

in a nontrivial context this study is also an attempt to get a better understanding of the phase diagram of the GNM itself.

This paper is organized as follows. In sect. 2 we will summarize some known properties of the continuum GNM that will be relevant for a discussion of the thermodynamics. In sect. 3 we discuss the setup of our lattice calculations and in sect. 4 we present the results of our Langevin simulations. Sect. 5 contains our conclusions.

2. The Gross-Neveu model

The GNM is a (1 + 1) dimensional renormalizable field theory for n_f species of Dirac fermions interacting through a 4-fermion term. The action is given by

$$\mathscr{S} = \sum_{j=1}^{n_f} \left[\bar{\psi}^{(j)} \partial\!\!\!/ \psi^{(j)} - \tfrac{1}{2} g^2 \left(\bar{\psi}^{(j)} \psi^{(j)} \right)^2 \right]. \tag{2.1}$$

The four-fermion term can be replaced by a quadratic term with the help of a real scalar field σ. This gives

$$\mathscr{S} = \sum_{j=1}^{n_f} \left[\bar{\psi}^{(j)} \partial\!\!\!/ \psi^{(j)} + \frac{1}{2g^2} \sigma^2 + \sigma \bar{\psi}^{(j)} \psi^{(j)} \right]. \tag{2.2}$$

The GNM is an asymptotically free theory with the first term of the β-function given by*

$$\beta(g) = -\frac{n_f - 1}{2\pi} g^3 + \mathrm{O}(g^5). \tag{2.3}$$

The action has a discrete chiral symmetry which is spontaneously broken, i.e. the scalar field σ takes on a nonvanishing vacuum expectation value σ_0 and gives a nonvanishing mass to the elementary fermion. In addition the GNM is known to have a sequence of (anti)fermion-(anti)fermion bound states below the threshhold for the kink-antikink state. In the large n_f limit the mass spectrum is thus given by [7]

$$m_1 = \sigma_0, \qquad \text{single-particle state}, \tag{2.4a}$$

$$m_n = \sigma_0 \frac{2n_f}{\pi} \sin\left(\frac{n}{n_f} \frac{\pi}{2} \right), \quad n = 2, \ldots, n_f - 1, \qquad n\text{-particle bound state}, \tag{2.4b}$$

$$m_s = \frac{2n_f}{\pi} \sigma_0, \qquad \text{kink-antikink}. \tag{2.4c}$$

* The second universal term in the β-function has been calculated recently [11]. We did not include it in our analysis since we feel that a second independent check of this involved calculation would be necessary.

In sect. 4 we will discuss the relation between the mass spectrum and the thermodynamics at $\mu \neq 0$. In particular we will see that in the zero temperature limit the chiral phase transition is triggered by the creation of a kink-antikink at rest. Kink-antikink states become increasingly important with lower temperature: The total number of fermions and/or antifermions in a kink-antikink state is n_f. From eq. (2.4c) it thus follows that the energy per constituent is $m_s/n_f = 2\sigma_0/\pi$ which is a factor $2/\pi$ smaller than the energy of a single particle state. In addition a kink-antikink state that contains only fermions has fermion number n_f. These states thus yield minimal energy configurations for a given total fermion number. The phase structure of the GNM has been analyzed in the $n_f \to \infty$ limit [8–10]. A mean field analysis of the continuum GNM suggests that at $\mu = 0$ there is a second order chiral transition at the critical temperature [8, 9]*

$$T_c = 0.5669\sigma_0 , \tag{2.5}$$

while it is first order at $T = 0$ with μ_c given by [10]

$$\mu_c \simeq 0.71\sigma_0 . \tag{2.6}$$

In the mean field calculations the transition switches from second to first order in the interior of the phase diagram at $(T/\sigma_0, \mu_c/\sigma_0) = (0.318, 0.608)$. However, the mean field calculation does not taken into account rapidly varying field configurations as is the case for the highly localized kink-antikink states. It has been shown that their contribution to the thermodynamics is exponentially suppressed at $\mu = 0$ in the $n_f \to \infty$ limit [9]. However we expect them to be relevant at nonzero μ. This may explain why the Langevin simulations we are going to discuss in this paper suggest that the chiral transition is first order for all $\mu \neq 0$ and second order only for $\mu \equiv 0$.

3. The Gross-Neveu model on the lattice

Different discretized versions of the GNM have been discussed by Cohen et al. [12]. We follow their discussion and use a lattice version of the GNM where the scalar field σ is defined on the plaquettes of a two-dimensional lattice**. This has the advantage that chiral symmetry is spontaneously broken at strong coupling as

* For finite n_f the chiral symmetry is restored at any nonzero temperature. The following discussion thus refers to the $n_f \to \infty$ limit of the GNM.

** The plaquette is labelled by the site index of its lower left corner.

well as at weak coupling. Using staggered fermions the lattice action becomes

$$S = \sum_{k=1}^{N} \sum_{i,j} \bar{\chi}^{(k)} Q_{ij} \chi^{(k)} + \frac{1}{2g^2} \sum_j \sigma_j^2 , \tag{3.1}$$

with the fermion matrix given by

$$Q_{ij} = \tfrac{1}{4}[\sigma_j + \sigma_{j-\hat{0}} + \sigma_{j-\hat{1}} + \sigma_{j-\hat{0}-\hat{1}}]\delta_{ij} + \tfrac{1}{2}\left[e^{\mu}\delta_{j,i+\hat{0}} - e^{-\mu}\delta_{j,i-\hat{0}}\right]$$

$$+ \tfrac{1}{2}\left[\delta_{j,i+\hat{1}} - \delta_{j,i-\hat{1}}\right](-1)^t . \tag{3.2}$$

Since the number of flavors is doubled in two dimensions the action, eq. (3.1), describes $n_f = 2N$ flavors in the continuum limit. We have introduced a chemical potential in the action through exponential factors $e^{\mu}(e^{-\mu})$ on links in the forward (backward) time direction of the lattice [3, 4].

Integrating over the Grassmann fields $\chi, \bar{\chi}$ the partition function can be written as

$$Z = \int \prod_i \mathrm{d}\sigma_i \, [\det Q]^N \exp\left(- \frac{1}{2g^2} \sum_i \sigma_i^2 \right). \tag{3.3}$$

The numerical analysis of the GNM model at $\mu \neq 0$ relies on the observation that the matrix Q is real. Thus all complex eigenvalues of the fermion matrix have to come in complex conjugate pairs. This insures us that $\det Q$ is almost always positive except on rare configurations which happen to have some real eigenvalues*. Unlike in the case of QCD [1] we can thus use standard stochastic techniques to simulate the GNM at finite density. We decided to use a Langevin algorithm which may also be useful for the case of complex actions [13]. The scalar field σ thus gets updated according to

$$\frac{\partial \sigma_j}{\partial t} = - \frac{\partial S_{\mathrm{eff}}}{\partial \sigma_j} + \eta_{j,t} , \tag{3.4a}$$

where

$$S_{\mathrm{eff}} = \frac{1}{2g^2} \sum_j \sigma_j^2 + N \, \mathrm{Tr} \ln Q , \tag{3.4b}$$

$\eta_{j,t}$ is random gaussian noise. To evaluate the derivative of S_{eff} in eq. (3.4a) we need the diagonal elements of the inverse fermion matrix. These matrix elements have been calculated exactly using standard matrix inversion routines. For two dimen-

* As the scalar field σ entering on the diagonal of the matrix Q is essentially random we expect these configurations to be of measure zero.

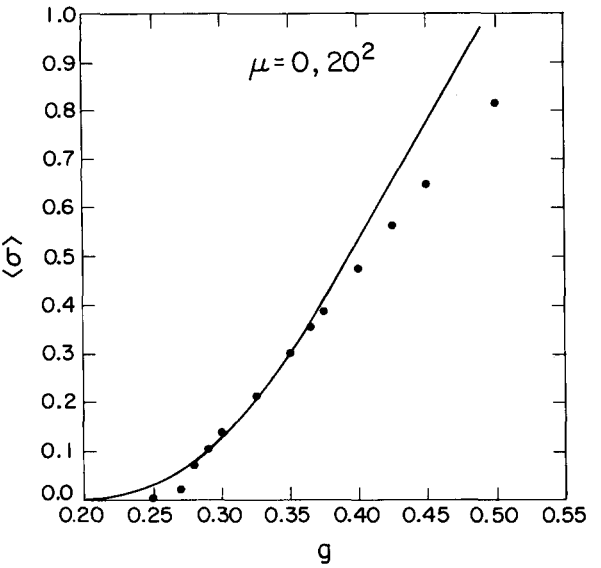

Fig. 1. Vacuum expectation value σ_0 of the scalar field as a function of the bare coupling g. The lattice size is 20^2 and the number of fermion flavors is $n_f = 12$. The dashed curve shows the asymptotic scaling prediction, eq. (3.6).

sions this is still feasible even on fairly large lattices. The time derivative in the Langevin equation has been approximated using a second order Runge-Kutta scheme with finite time step $dt = 0.05$.

As we are interested in the thermodynamics of the $n_f \to \infty$ GNM, we should use a large value for n_f to approximate this limit. Guided by the analysis of the GNM in ref. [12] we choose $n_f = 12$ throughout our calculations. In order to compare our simulation with continuum results we have to work in the scaling regime of the lattice model. In fig. 1 we show the scaling behavior of the scalar field σ_0 on a 20^2 lattice

$$\sigma_0 = \langle \sigma \rangle_{\mu = 0, T = 0}. \tag{3.5}$$

A comparison with the asymptotic scaling relation

$$a\Lambda = \exp\left(-\frac{\pi}{n_f - 1} \frac{1}{g^2} \right) \tag{3.6}$$

indicates that the continuum regime is reached for $g < 0.4$. Below $g_c \simeq 0.28$ we observe a sudden drop in $\langle \sigma \rangle$ to a chiral symmetric ($\langle \sigma \rangle = 0$) phase. This is a finite temperature effect. On a lattice with $N_\tau = 20$ (temperature $T = 1/N_\tau$) we expect from eq. (2.5) that the chiral symmetry restoring transition occurs at a coupling g_c

at which the chiral condensate is given by

$$\sigma_0 = \frac{1}{0.5669 N_\tau} \tag{3.7}$$

on an infinite lattice. Thus for $N_\tau = 20$ we would expect the transition to occur at a coupling g_c at which $\sigma_0 \simeq 0.09$ for $T = 0$ ($N_\tau = \infty$). This is in agreement with the value extracted from the asymptotic scaling curve, shown in fig. 1, at $g_c \simeq 0.28$ and indicates that $n_f = 12$ is a good approximation to the $n_f \to \infty$ limit. A detailed analysis of the thermodynamics of the GNM is given in the next section.

4. Thermodynamics of the Gross-Neveu model

In this section we will analyze the phase structure of the GNM as a function of temperature $T = 1/N_\tau$ and chemical potential. In the $T \to 0$ limit we are interested in effects related to the discontinuous Fermi distribution function, which allows us to extract information about the mass spectrum of the GNM [7]. At $\mu \neq 0$, $T \neq 0$ we will concentrate on an analysis of the order of the chiral transition and compare with continuum mean field calculations [10]. Let us start with a discussion of the $\mu = 0$ case which has been previously analyzed in ref. [12].

4.1. $\mu = 0$, $T \neq 0$

The chiral transition has been discussed in ref. [12] for various values of n_f. There good agreement between the MC simulations and the expected continuum result, eq. (2.5), has been found on rather small lattices. In fig. 2 we show results for $\langle \sigma \rangle$ obtained on a 60×6 lattice with $n_f = 12$. A continuous chiral symmetry restoring transition occurs at

$$g_c = 0.3532 \pm 0.0025 . \tag{4.1}$$

From fig. 1 we see that this value lies well in the scaling region. The zero-temperature expectation value for the scalar field σ is given by $\sigma_0 \simeq 0.31 \pm 0.01$. Thus we get for the critical temperature

$$T_c = (0.53 \pm 0.03)\sigma_0 , \tag{4.2}$$

in good agreement with the $n_f \to \infty$ continuum result, eq. (2.5).

4.2. $\mu \neq 0$, $T \neq 0$

To study the phase diagram of the GNM in the μ, T plane we selected a coupling g in the scaling regime and varied the temperature by changing the temporal extent of the lattice. Thus simulations have been performed on lattices of

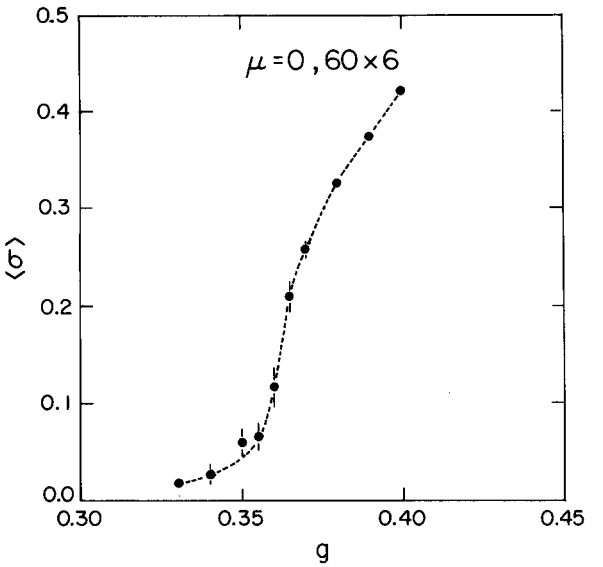

Fig. 2. σ_0 versus g on a 60×6 lattice for $n_f = 12$.

size $60 \times N_\tau$ with $N_\tau = 6$, 8, 10, 14 and 20. For each N_τ the chemical potential has been varied to determine the chiral transition point. The number of Langevin iterations per μ value varied from 5000–17 000. In figs. 3 and 4 we show results for $\langle \sigma \rangle$ and the fermion number density

$$n = \frac{\partial}{\partial \mu} \ln Z. \tag{4.3}$$

For large N_τ (small T) the existence of a first order transition is evident and in agreement with continuum results. To analyze the order of the transition at higher temperatures we performed long runs in the critical region and studied the distribution of the scalar field expectation value. In figs. 5a–c we show results for $N_\tau = 6$, 8 and 10, which clearly suggest that in all cases the chiral transition is first order. The resulting phase diagram in the μ, T and n, T planes is shown in fig. 6.

What is the physics of the two phases? At small μ states with large fermion number are suppressed and light particles contribute predominantly to the thermodynamics. At large μ, however, states with large fermion number are favored. Thus we expect that the low density phase is well described by a free Fermi gas with fermions of mass $m = \sigma_0 = \langle \sigma \rangle_{\mu=0,\, T=0}$, while the high density phase consists of a condensate of kink-antikinks and thus may be approximated by a gas of fermions with mass

$$m = \frac{m_s}{n_f} = \frac{2}{\pi} \sigma_0. \tag{4.4}$$

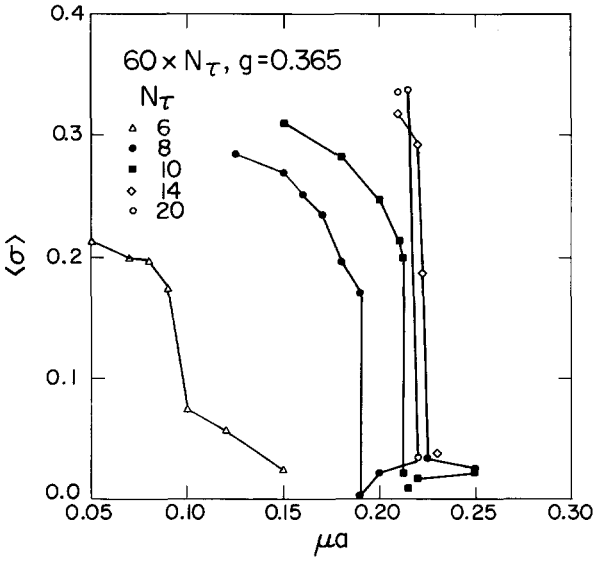

Fig. 3. $\langle \sigma \rangle$ versus μ at $g = 0.365$ on lattices of size $60 \times N_\tau$, $N_\tau = 6, 8, 10, 14$ and 20.

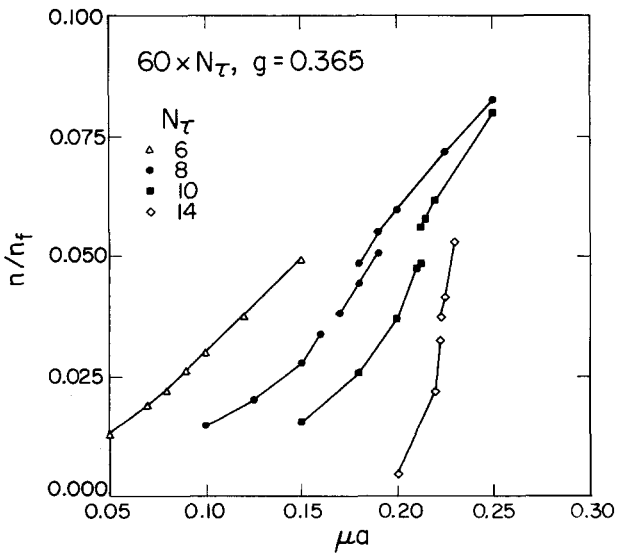

Fig. 4. Fermion number density divided by the number of flavors as a function of μ at $g = 0.365$ on lattices of size $60 \times N_\tau$, $N_\tau = 6, 8, 10$, and 14.

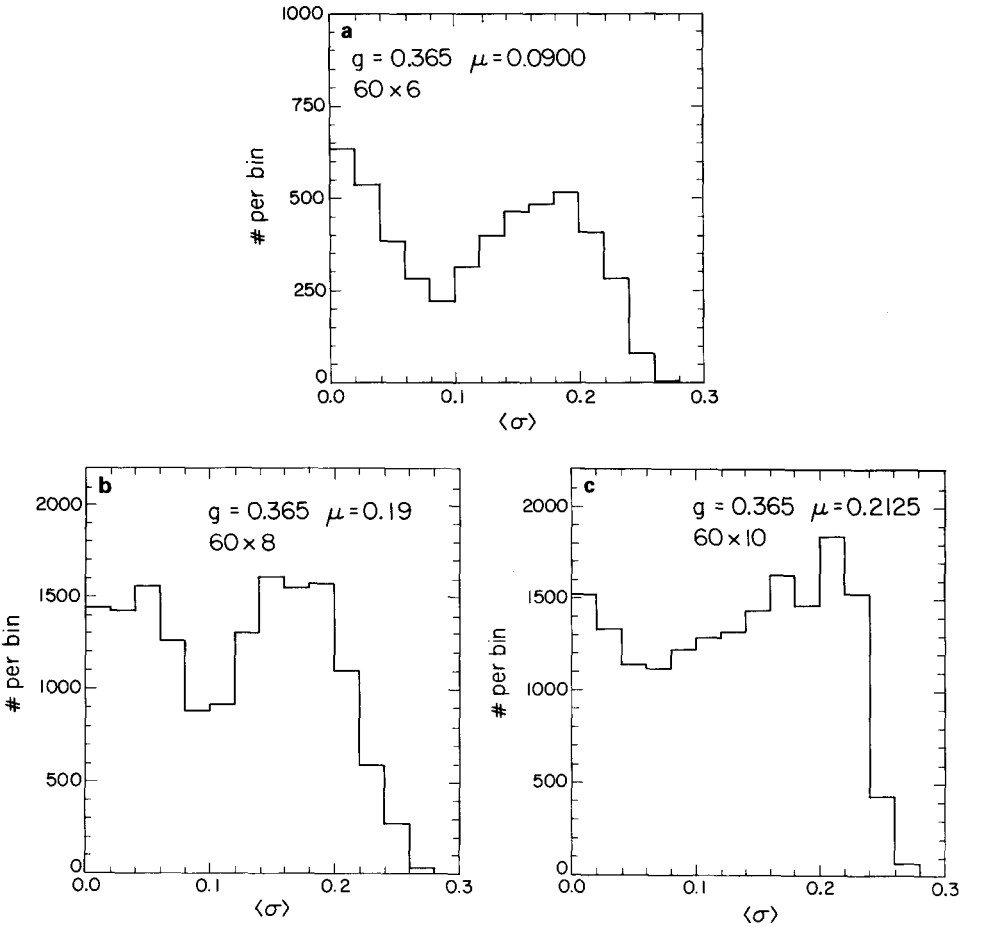

Fig. 5. Coexisting states at μ_c on lattices of size $N_\tau = 6$(a), 8(b), 10(c). Shown is the distribution of $|\Sigma_x \sigma_x|/V$. The total number of iterations is indicated in the figures. The first 1000 iterations have been neglected for equilibration.

In fig. 7 we compare the results for the number density at $N_\tau = 10$ with these approximations. There we take into account the temperature dependence of the scalar field expectation value by replacing σ_0 by $\langle\sigma\rangle$ measured at (μ, T). Apparently this yields a very good description of the different phases and seems to explain the size of the measured gap in the number density at (μ_c, T_c) shown in fig. 6b. Thus we conclude that the chiral transition is due to the formation of a kink-antikink condensate and seems to be first order for all $\mu \neq 0$.

4.3. $\mu \neq 0$, $T = 0$

From the analysis of the GNM at $T \neq 0$ we concluded that the chiral transition is triggered by the formation of kink-antikink pairs. With decreasing temperature

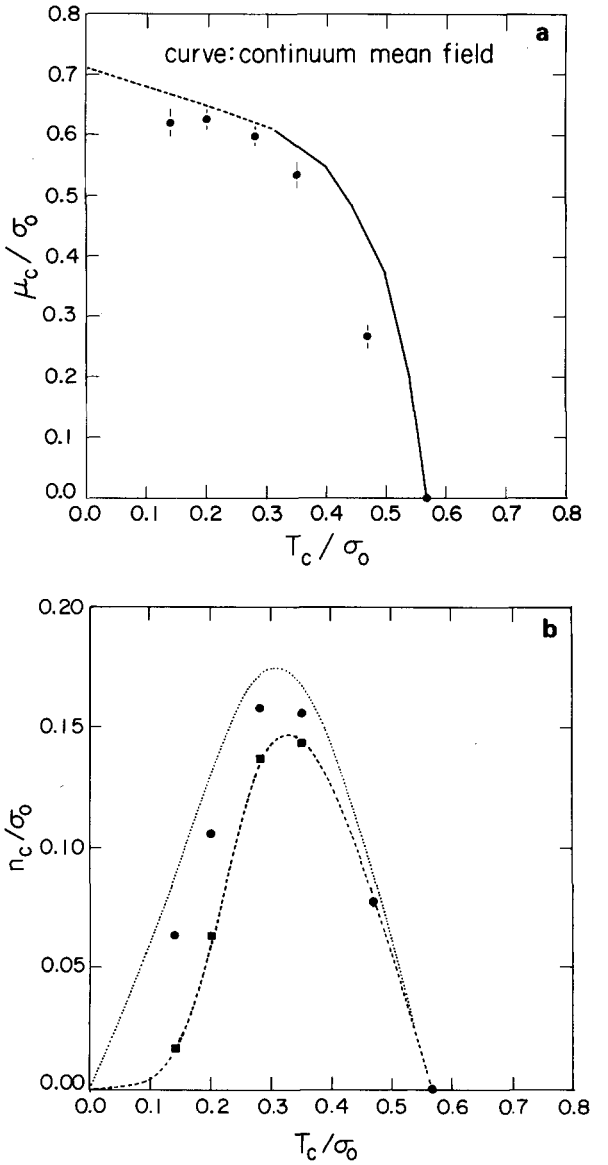

Fig. 6. Phase diagram of the Gross-Neveu model in the temperature-chemical potential plane (fig. 6a) and the temperature-density potential plane (fig. 6b). The dots show the critical parameter extracted from figs. 3 and 4. The curve in fig. 6a indicates the continuum mean field result of ref. [10]. The dashed curve indicates the region of first-order transitions while the solid curve corresponds to second-order transitions. The dashed(dotted) curves in fig. 6b show critical densities obtained from free Fermi lattice models with fermion mass $m = \langle\sigma\rangle_{\mu=\mu_c}(2/\pi\langle\sigma\rangle_{\mu=\mu_c})$ as explained in the text.

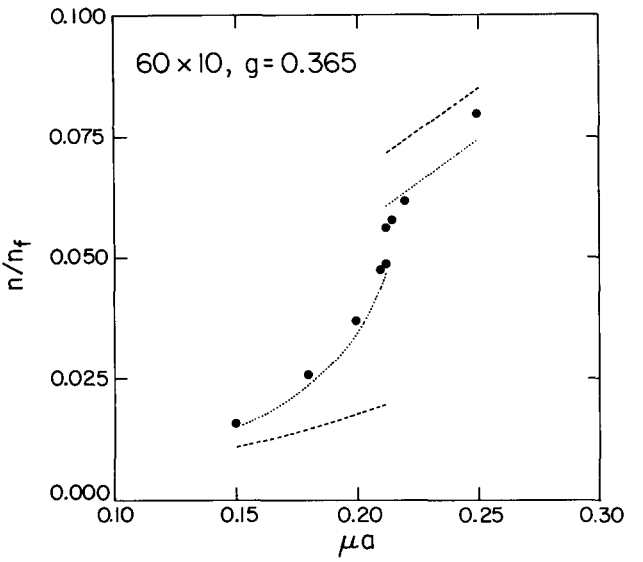

Fig. 7. n/n_f versus μ for $g = 0.365$ on a 60×10 lattice. The dots show Langevin data. The dashed curve shows the density for a free Fermi lattice gas with fermion mass $m = \sigma_0$ below μ_c and $m = 0$ above μ_c as input. The dotted curve gives improved Fermi gas calculations with σ_0 replaced by $\langle\sigma\rangle_{\mu,T}$ below μ_c and $(2/\pi)\langle\sigma\rangle_{\mu_c,T_c}$ above μ_c.

these states gain more and more weight in the partition function since they lead to configurations with minimal energy for a given fixed fermion number. At $T = 0$ the Fermi distribution function degenerates to a θ-function, leaving all states with energy larger than the Fermi energy unoccupied. Already from fig. 4 we see that with decreasing temperature the number density is essentially zero below a certain threshold value μ_0. Only for $\mu > \mu_0$ is the Fermi energy large enough that states with finite fermion number can be occupied in the $T \to 0$ limit. The kink-antikink is the state with smallest energy per constituent. We thus expect these to be occupied first and thus μ_0 is expected to be given by

$$\mu_0 = \frac{2}{\pi}\sigma_0 . \tag{4.5}$$

In fig. 8 we show a measurement of the number density on a 20^2 ($T \simeq 0$) lattice for various couplings. The existence of a threshold value μ_0 at which n starts becoming nonzero is clearly visible. Using the results for σ_0 shown in fig. 1 we obtain μ_0/σ_0 which is shown in fig. 9. Thus we see that indeed the ratio μ_0/σ_0 approaches the expected value $2/\pi$ in the scaling regime*. The relevance of kink-antikink config-

* For couplings which are too small we expect finite temperature effects to start setting in again leading to deviations from the expected value $2/\pi$.

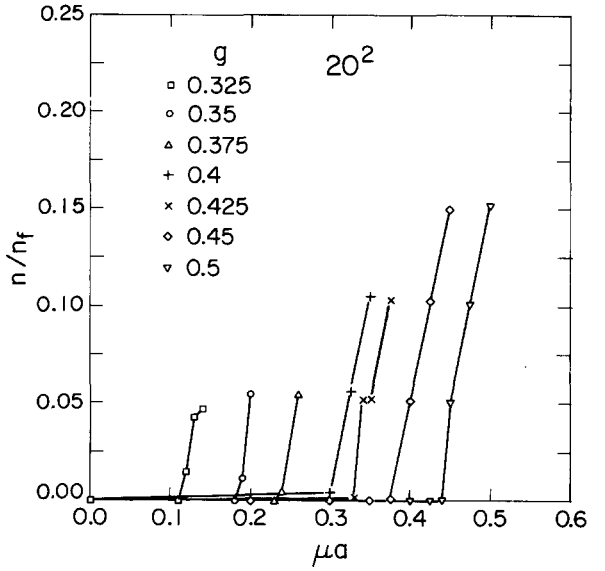

Fig. 8. n/n_f versus μ on a 20^2 lattice at various values of g as given in the figure.

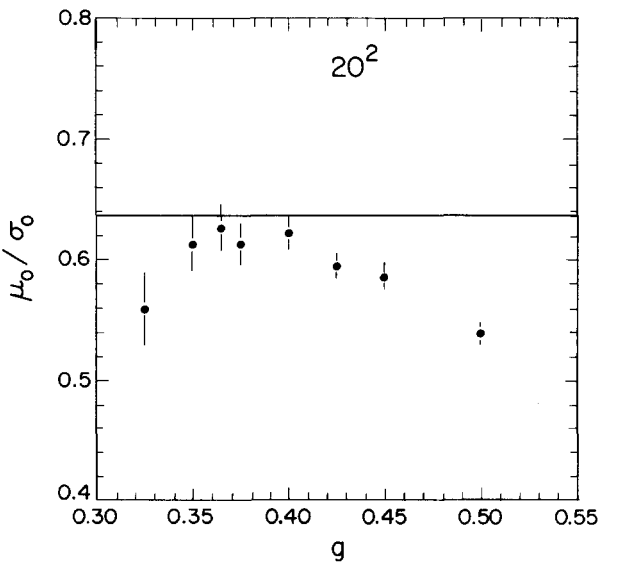

Fig. 9. μ/σ_0 versus g. σ_0 is taken from fig. 1 and μ_0 is the threshold value extracted from fig. 8. The dashed curve shows the expected value $2/\pi$.

urations can be observed directly by plotting the two-dimensional scalar field configurations. In fig. 10a we show a typical configuration an a 20^2 lattice at $g = 0.5$ and $\mu = 0.45$ which is close to the threshold value $\mu_0 = 0.44$ at this coupling value. A kink-antikink is clearly visible. Notice that the configuration is approximately time independent, i.e. $\sigma_{x,t} \simeq \sigma_{x,1}$ for all t. In fig. 10b we show a projection of

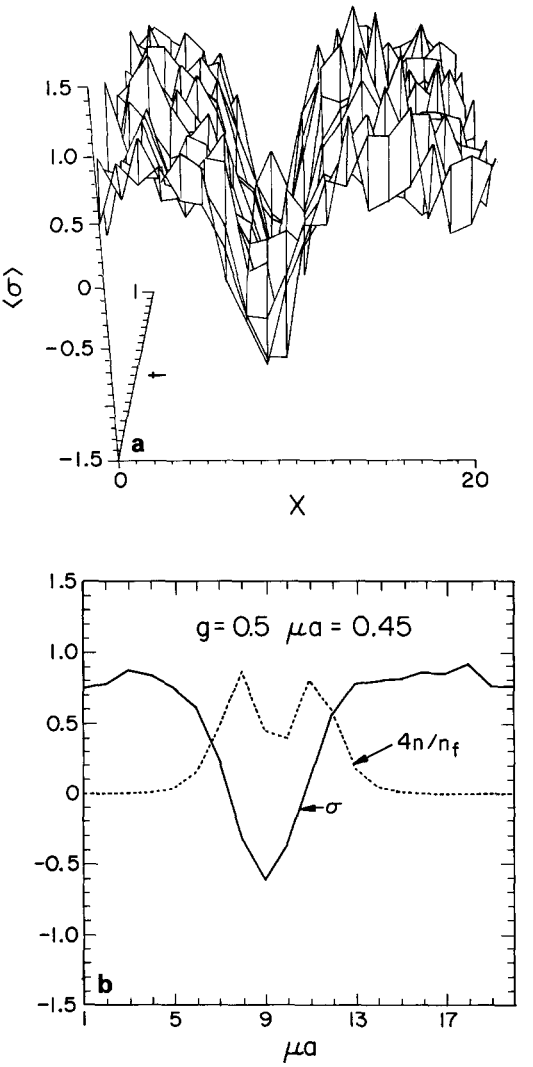

Fig. 10. Kink-antikink field configuration on a 20^2 lattice at $g = 0.5$, $\mu = 0.45$ (fig. 10a). Fig. 10b shows a projection of this configuration on the x-axis (solid curve) and the spatial distribution of the number density in this configuration.

this configuration onto the $t = 1$ axis

$$\sigma(x) = \sum_{t=1}^{20} \sigma_{x,t}, \tag{4.6}$$

along with the spatial distribution of the number density for this configuration. One sees that the fermions are localized in the kink and antikink. Integration of the number density yields

$$N_F = \sum_{x=1}^{20} n(x) = 12.06 \tag{4.7}$$

for this configuration. The number of fermions indeed equals n_f as expected.

5. Conclusions

We have analyzed the thermodynamics of the $n_f \to \infty$ Gross-Neveu model on the lattice. The lattice Langevin simulations at $\mu \neq 0$, $T \neq 0$ allow us to extract the phase diagram of the model in the scaling regime. The Langevin data suggest that the chiral transition is second order for $\mu \equiv 0$ but first order for all $\mu > 0$. This is in contrast to continuum mean field calculations [10]. The transition is found to be due to the creation of a kink-antikink condensate. This may explain the discrepancy between Langevin simulations and mean field, as the latter misses the influence of space dependent field configurations.

The analysis of the GNM at $\mu \neq 0$ shows that the latter formulation of field theories with nonvanishing chemical potential can provide an accurate description of the continuum theory and is sensitive to details of the mass spectrum of the theory. We thus expect interesting results from an analysis of QCD at $\mu \neq 0$ once the apparent numerical problems related to the appearance of a complex fermion determinant are under control.

This work was supported by the National Science Foundation under the grant NSF-PHY-82-01948. We gratefully acknowledge the National Center for Supercomputing Applications at Urbana-Champaign where the computations presented in this paper were performed.

References

[1] I. Barbour, N.E. Behilil, E. Dagotto, F. Karsch, A. Moreo, M. Stone and H.W. Wyld, Nucl. Phys. B275 [FS17] (1986) 296
[2] P.E. Gibbs, University of Glasgow preprint
[3] J. Kogut, H. Matsuoka, M. Stone, H.W. Wyld, S. Shenker, J. Shigemitsu and D.K. Sinclair, Nucl. Phys. B225 [FS9] (1983) 93
[4] P. Hasenfratz and F. Karsch, Phys. Lett. 125B (1983) 308

[5] R.V. Gavai, Phys. Rev. D32 (1985) 519
[6] D.J. Gross and A. Neveu, Phys. Rev. D10 (1974) 3235
[7] R. Dashen, B. Hasslacher and A. Neveu, Phys. Rev. D12 (1975) 2443
[8] L. Jacobs, Phys. Rev. D10 (1974) 3956;
B. Harrington and A. Yildiz, Phys. Rev. D11 (1975) 779
[9] R. Dashen, S.K. Ma and R. Rajaraman, Phys. Rev. D11 (1975) 1499
[10] U. Wolff, Phys. Lett. 157B (1985) 303
[11] W. Wetzel, Phys. Lett. 153B (1985) 297
[12] Y. Cohen, S. Elitzur and E. Rabinovici, Phys. Lett. 104B (1981) 289; Nucl. Phys. B220 [FS8] (1983) 102
[13] F. Karsch and H.W. Wyld, Phys. Rev. Lett. 55 (1985) 2242